



Published in final edited form as:

Science. 2022 April 29; 376(6592): 483–491. doi:10.1126/science.abn2479.

Molecular and neural basis of pleasant touch sensation in mice

Benlong Liu^{1,2,†}, Lina Qiao^{1,2,6,†}, Kun Liu^{1,2,7,†}, Juan Liu^{1,2}, Tyler J. Piccinni-Ash^{1,2}, Zhou-Feng Chen^{1,2,3,4,5,*}

¹Center for the Study of Itch and Sensory Disorders, Washington University School of Medicine, St. Louis, MO 63110, U.S.A.

²Department of Anesthesiology, Washington University School of Medicine, St. Louis, MO 63110, U.S.A.

³Department of Medicine, Washington University School of Medicine, St. Louis, MO 63110, U.S.A.

⁴Department of Psychiatry, Washington University School of Medicine, St. Louis, MO 63110, U.S.A.

⁵Department of Developmental Biology, Washington University School of Medicine, St. Louis, MO 63110, U.S.A.

⁶Present address: Department of Biochemistry and Molecular Biology, Institute of Acupuncture and Moxibustion, China Academy of Chinese Medical Sciences, Beijing, 100700, China.

⁷Present address: Department of Physiology, Institute of Acupuncture and Moxibustion, China Academy of Chinese Medical Sciences, Beijing, 100700, China.

Abstract

Pleasant touch provides emotional support that helps mitigate social isolation and stress. However, the underlying mechanisms remain poorly understood. Using a pleasant touch-conditioned place preference (PT-CPP) test, we show that genetic ablation of spinal excitatory interneurons expressing prokineticin receptor 2 (PROKR2), or its ligand PROK2 in sensory neurons, abolished PT-CPP without impairing pain and itch behaviors in mice. Mutant mice displayed profound impairment in stress response and prosocial behaviors. PROKR2 neurons responded most vigorously to gentle stroking and encode reward value. Collectively, we identify PROK2 as a long-sought neuropeptide that encodes and transmits pleasant touch to spinal PROKR2 neurons. The findings may have important implications for elucidating mechanisms by which pleasant touch deprivation contributes to social avoidance behaviors and mental illness.

One Sentence Summary:

*Corresponding author. chenz@wustl.edu.

†These authors contributed equally.

Author contributions: B. L. performed immunostaining, genetic ablation and electrophysiological studies, L. Qiao and K. Liu developed the PT-CPP test and performed *in vivo* extracellular recording. J. L. performed RNAscope and double staining. T.P.A participated in the behavioral test. B. L., L. Qiao and Z.F.C wrote the manuscript and Z.F.C conceived and supervised the project.

Competing interests: The authors declare no competing interests.

Data and materials availability: All data is available in the main text or supplementary materials.

Identification of a neuropeptide and spinal neural circuit that encode and transmit pleasant touch sensation.

Our sense of touch is composed of discriminative and affective components. While discriminative touch detects physical properties of tactile stimuli (e.g., location, shape, texture and force etc), affective touch conveys emotional value that is modulated by social context (1, 2). Pleasant touch (e.g., cuddling, caressing, patting) encodes positive hedonic information that facilitates emotional developmental, affiliative behavior, and well-being of social animals (1, 3, 4). Social touch is one of the most favored activities that might be evolutionarily conserved throughout the animal kingdom (5-7). In nonhuman primates and rodents, social or allogrooming behavior is important for strengthening and maintaining social bonding, reciprocity, attachment and hierarchy (8-10). Acute social isolation increases social cravings and reward-seeking behavior, while long-term deprivation of maternal care and positive social touch has lasting negative consequences on the emotional, behavioral and psychological development of social animals (11), including rodents (12, 13), infant rhesus monkeys (5) and children (14, 15). Indeed, affective touch avoidance/deficiency is one of the hallmarks of several neuropsychiatric disorders (e.g., autism spectrum disorders (16-19)). C tactile (CT) fibers innervating hairy skin encode positive valence of social touch in humans (1, 20-24), while *MrgprB4*-expressing sensory neurons and *Gpr83*-expressing spinal projection neurons have been implicated in mice (25, 26). Despite its profound importance, how pleasant touch information is encoded and transmitted from somatosensory neurons to the spinal cord remains unknown. Our understanding of molecules and neural circuits of pleasant touch has been hampered by a paucity of suitable animal models and methodologies that permit accurate inference and assessment of the affective state of mice that experience pleasant touch. Unlike discriminative touch, affective touch mediated by unmyelinated C fibers is a slow process (1). We postulated that pleasant touch is encoded by slow-acting neuropeptides in C fibers and their cognate excitatory G protein-coupled receptors (GPCR) in laminae II of the spinal cord that consists of microcircuits for relaying discrete sensory modalities, from primary afferents to the brain (27). In a search for lamina-specific GPCRs, we found that PROKR2 is expressed in lamina II of the spinal cord. Using a novel unbiased behavioral paradigm, in combination with physiological tests, extracellular recording and genetic approaches, we sought to examine the role of the PROKR2-PROKR2 signaling in pleasant touch.

Results

Properties of spinal PROKR2-expressing lamina II excitatory interneurons

We used *Prokr2*^{GFP} transgenic mice as a surrogate to characterize PROKR2 expression in the spinal cord. RNAscope in situ hybridization (ISH) followed by immunohistochemical (IHC) studies indicated that GFP of *Prokr2*^{GFP} mice recapitulates a large part of *Prokr2* expression in lamina II (80.4%) of the spinal cord (Fig. 1A to E). A significant fraction of GFP is distributed in the dorsal side of lamina II innervated by isolectin B4 binding (IB4) nonpeptidergic fibers (Fig. 1C). *Prokr2* is largely colocalized with the excitatory genes like vesicular glutamate transporter 2 (*Vglut2*, 94.1%) and *Lmx1b* (96.8%), but rarely overlaps with the inhibitory neuronal markers such as vesicular GABA transporter (*Vgat*, 6.4%) or

Pax2 (3.1%) (Fig. 1B and E; fig. S1A and B). RNA ISH and IHC showed that *Prokr2* rarely overlaps with gastrin-releasing peptide receptor (*Gpr*, 7.8%), an itch-specific receptor expressed in laminae I-II interneurons (28, 29), or PKC γ (5.7%) that labels the ventral side of lamina II inner (IIi) layer, with *Gpr83* (7.0%) or NK1R, two markers expressed in distinct subsets of projection neurons implicated in pleasant touch and pain, respectively (25) (Fig. 1B, C and E). To identify the downstream target of PROKR2 neurons, we next performed Cre-dependent virus-mediated anterograde monosynaptic tracing in the spinal cord of *Prokr2*^{Cre} mice using HSV-dTK-LSL-tdTomato as the monosynaptic tracer to follow the output neurons (Fig. 1F). RNAscope ISH or IHC revealed that approximately 85.5% of the output neurons labeled by tdTomato express *Gpr83*, whereas only 8.5% of which express NK1R (Fig. 1G and H).

We next examined whole-cell patch-clamp recordings of spinal cord slices obtained from *Prokr2*^{GFP} mice. The firing pattern of most *Prokr2*^{GFP} neurons was very homogenous: approximately 92.4% displayed initial bursting firing, with a few neurons showing single spike firing (Fig. 1I to K). To identify the type of peripheral sensory inputs, we recorded the response of *Prokr2*^{GFP} neurons in the parasagittal section of spinal slices obtained from *Prokr2*^{GFP} mice with the dorsal root (L4~L5) attached using the dorsal root stimulation method as described previously (Fig. 1L) (30). *Prokr2*^{GFP} neurons predominantly receive monosynaptic and polysynaptic C fiber inputs (a combined 85.4%) with a small fraction of polysynaptic A δ (4.9%) or A β inputs (9.8%) (Fig. 1M and N). Furthermore, PROKR2 application evoked subthreshold depolarizations in most *Prokr2*^{GFP} neurons, which was blocked by PKRA7, a PROKR2 antagonist (fig. S1C and D).

PROKR2 neurons are dispensable for pain and itch transmission

To assess the function of spinal PROKR2 neurons, we first validated *Prokr2*^{Cre} mice by intraspinal injection of Cre-dependent YFP virus. Most *Prokr2*^{Cre} neurons expressed YFP (81.2%) (Fig. 2A to C). We then employed an intersectional genetic strategy to ablate spinal PROKR2 neurons in *Prokr2*^{Cre} mice, hereafter referred to as ABL mice, as previously described (30) (Fig. 2D to F; fig. S2A and B). The specificity of ablation was demonstrated by the loss of most *Prokr2*^{Cre} neurons (84.9%) without affecting PKC γ , NKB, *Gpr* in the spinal cord or *Prokr2*^{GFP} in discrete brain regions (Fig. 2D to F; fig. S2C and D; fig. S3). A battery of pain and itch tests was conducted to assess the role of *Prokr2*^{Cre} neurons in somatosensory transmission. We did not observe statistically significant differences in thermal pain, cold pain, mechanical thresholds, as well as inflammatory pain induced by capsaicin between ABL mice and their littermate control mice (referred to as wild-type (WT) mice; Fig. 2G to K). Chemical and mechanical itch and the hairy skin sensitivity to a sticky tape of ABL mice were comparable to WT mice (Fig. 2L; fig. S2E and F).

PROKR2 neurons convey pleasant touch sensation

As a weak stimulus, gentle stroking with a soft brush on hairy skin of mice does not elicit a robust motor response that can be used as a proxy to quantify pleasant touch sensation. Moreover, using a hand or soft brush to simulate pleasant touch in mice often causes avoidance behavior without habituation and conditioning. To circumvent these confounds, we developed a novel protocol that includes two procedural features to avoid stress/anxiety

associated with handling. First, given that social isolation increases the urge for social touch/attachment (31), mice were single-housed for one week followed by week-long daily stroking sessions in the homecage. This procedure conditioned mice into a quiescent or inactive state upon gentle stroking, akin to pets being groomed (Fig. 3A and B; movies S1 to S3). Second, to increase the motivational drive to obtain rewards associated with pleasant touch (32), we performed eight conditioning sessions (one session/two days) using an unbiased two-chamber PT-CPP apparatus in which WT mice displayed no preference for either chamber (Fig. 3A; fig. S4B; movie S4). On the test day, we performed PT-CPP test to evaluate whether mice would spend more time in the chamber paired with gentle stroking than without. Indeed, both male and female mice developed PT-CPP as they spent significantly more time in the chamber paired with a soft brush (fig. S4A, C and D). These results demonstrate that gentle stroking in mice encodes the positive valence or hedonic value. In striking contrast to WT mice, ABL mice completely failed to show PT-CPP (Fig. 3C and D), indicating a profound loss of pleasant touch sensation. If PROKR2 neurons convey pleasant touch, their direct activation, in the absence of either primary afferent input or behavioral conditioning/context, should be positively reinforcing. We injected Cre-dependent ChR2 or eYFP virus intraspinally into *Prokr2*^{Cre} mice followed by the real-time place preference test (RTPP) using optogenetics (Fig. 3G). Consistently, *Prokr2*^{Cre-ChR2} mice preferred the chamber paired with photostimulation of PROKR2 neurons (5 and 10 Hz), whereas *Prokr2*^{Cre-eYFP} mice showed no preference (Fig. 3H and I). Together, these results demonstrate that PROKR2 neurons encode positive valence and rewarding value.

Apart from pleasant sensation (1), gentle stroking on the hairy skin of humans decreases heart rate (33) and acute thermal pain (34), reflecting a soothing state with a reduced level of stress (e.g., increasing the threshold for thermal pain). To ascertain whether mice might develop similar physiological changes, we measured the heart rate, thermal pain and stress hormone after gentle stroking. Indeed, mice showed significantly reduced heart rate, increased thermal pain threshold and reduced plasma corticosterone levels (fig. S4E to G). Consistent with behavioral studies, ABL mice displayed no significant reduction of the heart rate or analgesic effect in response to gentle stroking (Fig. 3E and F). The lack of behavioral and physiological changes in ABL mice further demonstrates the crucial role of PROKR2 neurons in conveying pleasant touch.

Neurophysiological features of PROKR2 neurons in response to varying stimuli

To interrogate neural correlates of pleasant touch, we performed *in vivo* extracellular recording of the response of spinal PROKR2 neurons to gentle stroking using a soft brush moving across the receptive field in the hairy skin of the hindlimb of *Prokr2*^{Cre;Ai32} mice expressing channelrhodopsin 2-eYFP (ChR2-eYFP) (Fig. 4A). Opto-tagged spinal neurons were classified as spinal *Prokr2*^{ChR2} neurons if they displayed reliable action potentials with a short response latency (10 ms) upon the delivery of a brief pulse of blue light (Fig. 4B) (35). Notably, the response of *Prokr2*^{ChR2} neurons was most vigorous when the hairy skin of mice was brushed at a slowly moving speed (18~22 cm/s); however, their firing became sluggish if the stroking speed was slower (2~3 cm/s) or faster (37~45 cm/s) (Fig. 4C and D). The mean firing rates at three brushing speeds exhibited an inverted U shape (Fig. 4E), reminiscent of that of human CT fibers (22, 23). This prompted us to examine whether

other features of *Prokr2^{ChR2}* neurons may resemble the hallmarks of human CT fibers (1, 21, 22, 24). One signature of CT fibers is that they show no preference for orientation in the receptive field (24). Indeed, *Prokr2^{ChR2}* neurons displayed comparable firing rates, irrespective of stroking directions (e.g., from rostral to caudal or from left to right, Fig. 4F to H). Another unique feature is fatigue to repetition of brush stroking, referring to gradually attenuated responses to repeated stroking stimuli within seconds (1, 21, 22, 24). This feature distinguishes unmyelinated CT fibers from myelinated low-threshold mechanoreceptors (23) and has also been observed in cutaneous C mechanoreceptor afferents in rats (36) and cats (37). The firing rate of *Prokr2^{ChR2}* neurons also exhibited fatigue to repeated brush stroking and was reduced by 40.7~78.8% within 10 series of successive brush stroking (2 s interval) (Fig. 4I and J).

At last, we examined several non-gentle stroking related stimuli that could elicit the response of CT fibers (21, 38). Consistently, *Prokr2^{ChR2}* neurons responded to punctate stimulation (von Frey filament at 0.07 g or 0.7 mN), pinprick stimulation and cooling temperature (30°~15°) (fig. S5A to C).

Coding of pleasant touch by PROK2 in sensory neurons

We next examined *Prok2* expression in several types of dorsal root ganglion (DRG) neurons using RNAscope combined with IHC. *Prok2* partially overlaps to varying degrees with TRPV1 and CGRP which are expressed in nociceptive neurons, IB4, NF200, a neurofilament expressed predominantly in large-diameter neurons, *MrgprB4* (26) and tyrosine hydroxylase expressed in some C-LTMRs (39) (Fig. 5A and B, fig. S6F). Overall, approximately 59.6% of DRG neurons express *Prok2*. To ascertain whether *Prok2*-expressing primary afferents form monosynaptic contacts with PROKR2 neurons, we performed rabies virus-mediated retrograde tracing in the spinal cord of *Prokr2^{Cre}* mice (30) (fig. S6A and B). Examination of *Prok2* expression with retrograde transported RVdG that labels the input neurons with dsRed in DRGs revealed that approximately 70% of the input neurons were co-labeled with *Prok2* (fig. S6C to E). Only a small portion of CGRP fibers and minimal TRPV1 fibers formed direct contacts with PROKR2 neurons, whereas no *MrgprB4* afferents were found to form monosynaptic contacts with PROKR2 neurons (fig. S6C and D). Further, we show that the sizes of *Prok2* input neurons normally are in 200 to 400 μm^2 range, indicating that they are small DRG neurons (fig. S6E).

To determine the role of PROK2 in pleasant touch, we generated mice harboring a floxed allele of *Prok2* using the gene targeting strategy (Fig. 5C). Floxed *Prok2* mice were bred with *Nav1.8^{Cre}* mice, which express the Cre recombinase in small nociceptive sensory neurons, to delete *Prok2* in *Nav1.8^{Cre}* neurons of DRGs (Fig. 5C). The expression of *Prok2* was reduced by 52.8% without affecting IB4, CGRP, *MrgprB4* in DRGs and IB4, CGRP central fibers in the lumbar cord (Fig. 5C to E; fig. S7A to D). Mice with conditional knockout of *Prok2* in DRGs, referred to as *Prok2* CKO mice, failed to show PT-CPP (Fig. 5F to H). By contrast, they showed normal pain and itch behaviors (Fig. 5K to O). Furthermore, *Prok2* CKO mice did not show a significant change in the heart rate and thermal pain thresholds after gentle stroking (Fig. 5I and J). CT and C-LTMRs are insensitive to capsaicin that activates TRPV1 fibers (20, 40). This prompted us to explore

the role of TRPV1 fibers in pleasant touch. Ablation of the central terminals of TRPV1 fibers with intrathecal resiniferatoxin (RTX), a potent TRPV1 agonist, abolished neurogenic pain elicited by capsaicin and markedly attenuated mechanical itch that is dependent on A β -LTMR/C fiber inputs and GRPR neurons (27, 30) (fig. S8A to D). Strikingly, RTX treatment had no effect on PT-CPP (fig. S8E to G).

Profound deficits in stress response and prosocial behaviors of PROK2 mutant mice

Pleasant social touch affords tremendous emotional and psychological benefits by indirectly activating the endogenous reward/pleasure circuits to release a plethora of neuropeptides and neurotransmitters that encode anti-stress, positive hedonic and prosocial value (1, 8, 41-43). We sought to examine whether a loss of pleasant touch developmentally or in adult mice may result in abnormal stress responses. *Prok2*CKO mice spent significantly less time than their WT littermates in the center zone of the open-field apparatus, in the light illuminated chamber of the light-dark box and in the open quadrants of the elevated zero maze apparatus (Fig. 6A to C). By contrast, the time ABL mice spent in these areas did not differ from their WT littermates (Fig. 6A to C). We further assessed social novelty recognition of mutant mice using the three-chamber social interaction test. Unlike WT mice, neither *Prok2*CKO nor ABL mice displayed a preference for a novel mouse, demonstrating severe deficits in social novelty recognition (Fig. 6D; fig. S9).

At last, we evaluated whether *Prok2*CKO or ABL mice might have deficits in social touch behavior. To examine this, we first monitored spontaneous social interactions between paired C57BL/6J adult mice in the homecage, which subserves a more naturalistic environment, and observed frequent social or allogrooming behavior unrelated to sexual or aggressive/conflict activity (Fig. 6E; movie S5). In sharp contrast to the paired WT-WT conspecifics, social grooming of WT mice towards ABL mice was significantly diminished (Fig. 6F). Unexpectedly, ABL mice rarely groomed WT conspecifics capable of sensing pleasant touch (Fig. 6F). These deficits were even more pronounced in the WT-*Prok2*CKO pairs (Fig. 6G).

Discussion

Using an interdisciplinary approach, our studies demonstrate the crucial function of the PROK2-PROKR2 signaling pathway in pleasant touch. The profound loss of pleasant touch sensation in *Prok2*CKO mice underscores the pivotal role of PROK2 in the coding and transmitting pleasant touch information. The finding that pleasant touch is conveyed by capsaicin-insensitive C fibers reveals parallel peptidergic pathways that convey positive and negative valence from the skin to the spinal cord, mirroring that from the spinal cord to the brain (25). We argue that PROK2 in A β /A δ fibers is unlikely to be involved in pleasant touch, as PROKR2 neurons receive no direct inputs from these fibers. Although PROK2 fibers that synapse with spinal PROKR2 neurons could be the equivalent of human CT fibers, it is not feasible to examine their conduction velocities or cutaneous innervation pattern in isolation. Nonetheless, remarkable neurophysiological features shared by PROKR2 neurons and human CT fibers indicate that a subset of PROK2 fibers is equivalent to CT fibers. The response of PROKR2 neurons to cooling temperature implies that PROKR2 neurons may be a convergent point for integrating different kinds of

cutaneous information that encodes positive hedonic valence (e.g., pleasantness of cooling). Importantly, these data support the neuropeptide code model that somatosensory modalities with slow response kinetics are encoded by neuropeptides in sensory neurons and conveyed by respective spinal microcircuits that can be defined and identifiable through unique GPCR expression (27). The development of the PT-CPP test that entails inference of pleasant touch in an unbiased manner overcomes a major obstacle in the interrogation of molecular underpinnings and neural circuits of pleasant touch. Together with the ethologically relevant semi-naturalistic social grooming paradigm, we provide a new avenue to unravel mechanisms by which the need for affective touch drives social attachment and affiliative behaviors.

The present study has important clinical implications. The heightened stress/anxiety-like behaviors of *Prok2* CKO but not ABL mice are attributable to a lack of pleasant touch experience during postnatal development, which supports previous studies suggesting that early tactile experience is more instrumental in shaping the resilience of offspring against stressful events (13, 44). Accordingly, ABL mice are less vulnerable to stress. In light of the challenge in the study of developmental role of pleasant touch due to the multisensory nature of parental care (45), *Prok2* CKO mice might serve as an invaluable animal model for assessment of the long-term effects of deprivation of maternal or caregiving's nurturing touch on offspring's health and prosocial behaviors. The failure of mutant mice to recognize novel conspecifics indicates that pleasant touch is also crucial for social recognition and social memory important for social bonding (46). In addition, the dramatic avoidance of the social touch phenotype is reminiscent of some early traits of ASD (11, 19, 47). Further analysis of prosocial behavioral impairment in PROK2 CKO mice may offer novel insights into the etiology of certain neurodevelopmental and affective disorders that hinder social interactions and affiliative behaviors. The inability of mutant mice to groom WT conspecifics underscores the function of PROK2 signaling in mediating synchronous and bidirectional communication of mutually beneficial social information through reciprocal tactile contacts (7). Finally, the striking observation that the firing features of PROKR2 neurons recapitulate the hallmarks of human CT fibers reinforces the notion that neural mechanisms of pleasant touch are conserved between humans and rodents. Conceivably, a deficiency of PROK2-PROKR2 signaling might result in social and emotional impairments that could lead to social isolation and mental disorders.

Supplementary Material

Refer to Web version on PubMed Central for supplementary material.

ACKNOWLEDGMENTS

We thank X. Liu for technical help, Y. Zhang and F. Gao for help with viral tracing; Q. Ma and M. Goulding for providing *Lbx1^{Flpo}* and *Tau^{ds-DTR}* lines; L. Setton, and T. McGrath for help with the initial design of the stroking test and R. Bardoni for discussion.

Funding:

The project has been supported by the NIH grants 1R01AR056318-06 and R01NS094344 (Z. F. C).

REFERENCES AND NOTES

1. McGlone F, Wessberg J, Olausson H, Discriminative and affective touch: sensing and feeling. *Neuron* 82, 737–755 (2014). [PubMed: 24853935]
2. Abraira VE, Ginty DD, The sensory neurons of touch. *Neuron* 79, 618–639 (2013). [PubMed: 23972592]
3. Morrison I, Loken LS, Olausson H, The skin as a social organ. *Experimental Brain Research* 204, 305–314 (2010). [PubMed: 19771420]
4. Montagu A, *Touching: The Human Significance of the Skin*. (HarperCollins New York, ed. 3rd ed, 1986).
5. Harlow HF, Suomi SJ, Nature of love--simplified. *Am Psychol* 25, 161–168 (1970). [PubMed: 4984312]
6. Panksepp J, *Affective Neuroscience: The foundations of human and animal emotions*. Davidson RJ, Ekman P, Scherer K, Eds., *Affective neuroscience* (Oxford University Press, New York, 1998), pp. 466.
7. Hertenstein MJ, Verkamp JM, Kerestes AM, Holmes RM, The communicative functions of touch in humans, nonhuman primates, and rats: a review and synthesis of the empirical research. *Genet Soc Gen Psychol Monogr* 132, 5–94 (2006). [PubMed: 17345871]
8. Dunbar RIM, The social role of touch in humans and primates: Behavioural function and neurobiological mechanisms. *Neurosci Biobehav R* 34, 260–268 (2010).
9. de Waal FBM, Suchak M, Prosocial primates: selfish and unselfish motivations. *Philos T R Soc B* 365, 2711–2722 (2010).
10. Wilson EO, *Sociobiology: The New Synthesis*. (Harvard University Press, Cambridge, Massachusetts., 1975).
11. Cascio CJ, Moore D, McGlone F, Social touch and human development. *Dev Cogn Neurosci* 35, 5–11 (2019). [PubMed: 29731417]
12. Hall FS, Social deprivation of neonatal, adolescent, and adult rats has distinct neurochemical and behavioral consequences. *Crit Rev Neurobiol* 12, 129–162 (1998). [PubMed: 9444483]
13. Kaffman A, Meaney MJ, Neurodevelopmental sequelae of postnatal maternal care in rodents: clinical and research implications of molecular insights. *J Child Psychol Psychiatry* 48, 224–244 (2007). [PubMed: 17355397]
14. Spitz RA, Hospitalism; an inquiry into the genesis of psychiatric conditions in early childhood. *Psychoanal Study Child* 1, 53–74 (1945). [PubMed: 21004303]
15. Bowlby J, Maternal care and mental health. *Bull World Health Organ* 3, 355–533 (1951). [PubMed: 14821768]
16. Tomchek SD, Dunn W, Sensory processing in children with and without autism: A comparative study using the short sensory profile. *Am J Occup Ther* 61, 190–200 (2007). [PubMed: 17436841]
17. Voos AC, Pelphrey KA, Kaiser MD, Autistic traits are associated with diminished neural response to affective touch. *Soc Cogn Affect Neurosci* 8, 378–386 (2013). [PubMed: 22267520]
18. Thyé MD, Bednarz HM, Herringshaw AJ, Sartin EB, Kana RK, The impact of atypical sensory processing on social impairments in autism spectrum disorder. *Dev Cogn Neurosci* 29, 151–167 (2018). [PubMed: 28545994]
19. Lai MC, Lombardo MV, Baron-Cohen S, Autism. *Lancet* 383, 896–910 (2014). [PubMed: 24074734]
20. McGlone F, Walker S, Ackerley R, in *Affective Touch and the Neurophysiology of CT Afferents*, Olausson H, Wessberg J, Morrison I, McGlone F, Eds. (Springer, New York, 2016), chap. 16, pp. 265–282.
21. Vallbo A, Loken L, Wessberg J, in *Affective touch and the neurophysiology of CT afferents*, Olausson H, Wessberg J, Morrison I, McGlone F, Eds. (Springer Nature, New York, 2016), chap. 1, pp. 1–30.
22. Loken LS, Wessberg J, Morrison I, McGlone F, Olausson H, Coding of pleasant touch by unmyelinated afferents in humans. *Nature neuroscience* 12, 547–548 (2009). [PubMed: 19363489]

23. Vallbo AB, Olausson H, Wessberg J, Unmyelinated afferents constitute a second system coding tactile stimuli of the human hairy skin. *J Neurophysiol* 81, 2753–2763 (1999). [PubMed: 10368395]
24. Wessberg J, Olausson H, Fernstrom KW, Vallbo AB, Receptive field properties of unmyelinated tactile afferents in the human skin. *J Neurophysiol* 89, 1567–1575 (2003). [PubMed: 12626628]
25. Choi S et al. , Parallel ascending spinal pathways for affective touch and pain. *Nature* 587, 258–263 (2020). [PubMed: 33116307]
26. Vrontou S, Wong AM, Rau KK, Koerber HR, Anderson DJ, Genetic identification of C fibres that detect massage-like stroking of hairy skin in vivo. *Nature* 493, 669–673 (2013). [PubMed: 23364746]
27. Chen ZF, A neuropeptide code for itch. *Nat Rev Neurosci* 22, 758–776 (2021). [PubMed: 34663954]
28. Sun YG, Chen ZF, A gastrin-releasing peptide receptor mediates the itch sensation in the spinal cord. *Nature* 448, 700–703 (2007). [PubMed: 17653196]
29. Sun YG et al. , Cellular basis of itch sensation. *Science* 325, 1531–1534 (2009). [PubMed: 19661382]
30. Chen S et al. , A spinal neural circuitry for converting touch to itch sensation. *Nat Commun* 11, 5074 (2020). [PubMed: 33033265]
31. Keverne EB, Martensz ND, Tuite B, Beta-endorphin concentrations in cerebrospinal fluid of monkeys are influenced by grooming relationships. *Psychoneuroendocrino* 14, 155–161 (1989).
32. Cunningham CL, Gremel CM, Groblewski PA, Drug-induced conditioned place preference and aversion in mice. *Nat Protoc* 1, 1662–1670 (2006). [PubMed: 17487149]
33. Pawling R, Cannon PR, McGlone FP, Walker SC, C-tactile afferent stimulating touch carries a positive affective value. *Plos One* 12, (2017).
34. Liljencrantz J et al. , Slow brushing reduces heat pain in humans. *Eur J Pain* 21, 1173–1185 (2017). [PubMed: 28263013]
35. Fadok JP et al. , A competitive inhibitory circuit for selection of active and passive fear responses. *Nature* 542, 96–100 (2017). [PubMed: 28117439]
36. Leem JW, Willis WD, Chung JM, Cutaneous Sensory Receptors in the Rat Foot. *J Neurophysiol* 69, 1684–1699 (1993). [PubMed: 8509832]
37. Iggo A, Cutaneous mechanoreceptors with afferent C fibres. *J Physiol* 152, 337–353 (1960). [PubMed: 13852622]
38. Nordin M, Low-threshold mechanoreceptive and nociceptive units with unmyelinated (C) fibres in the human supraorbital nerve. *J Physiol* 426, 229–240 (1990). [PubMed: 2231398]
39. Li L et al. , The functional organization of cutaneous low-threshold mechanosensory neurons. *Cell* 147, 1615–1627 (2011). [PubMed: 22196735]
40. Caterina MJ et al. , The capsaicin receptor: a heat-activated ion channel in the pain pathway [see comments]. *Nature* 389, 816–824 (1997). [PubMed: 9349813]
41. Uvnas-Moberg K, Handlin L, Petersson M, Self-soothing behaviors with particular reference to oxytocin release induced by non-noxious sensory stimulation. *Frontiers in Psychology* 5, (2015).
42. Morrison I, Keep Calm and Cuddle on: Social Touch as a Stress Buffer. *Adapt Hum Behav Phys* 2, 344–362 (2016).
43. Panksepp J, Herman BH, Vilberg T, Bishop P, DeEsquinazi FG, Endogenous opioids and social behavior. *Neurosci Biobehav Rev* 4, 473–487 (1980). [PubMed: 6258111]
44. Meaney MJ, Maternal care, gene expression, and the transmission of individual differences in stress reactivity across generations. *Annu Rev Neurosci* 24, 1161–1192 (2001). [PubMed: 11520931]
45. Dulac C, O'Connell LA, Wu Z, Neural control of maternal and paternal behaviors. *Science* 345, 765–770 (2014). [PubMed: 25124430]
46. Walum H, Young LJ, The neural mechanisms and circuitry of the pair bond. *Nature Reviews Neuroscience* 19, 643–654 (2018). [PubMed: 30301953]
47. Bales KL et al. , Social touch during development: Long-term effects on brain and behavior. *Neurosci Biobehav Rev* 95, 202–219 (2018). [PubMed: 30278194]

48. Stirling LC et al. , Nociceptor-specific gene deletion using heterozygous Nav1.8-Cre recombinase mice. *Pain* 113, 27–36 (2005). [PubMed: 15621361]
49. Barry DM et al. , Exploration of sensory and spinal neurons expressing gastrin-releasing peptide in itch and pain related behaviors. *Nat Commun* 11, 1397 (2020). [PubMed: 32170060]
50. Lund I, Lundeberg T, Kurosawa M, Uvnas-Moberg K, Sensory stimulation (massage) reduces blood pressure in unanaesthetized rats. *J Auton Nerv Syst* 78, 30–37 (1999). [PubMed: 10589821]
51. Cunningham CL, Ferree NK, Howard MA, Apparatus bias and place conditioning with ethanol in mice. *Psychopharmacology (Berl)* 170, 409–422 (2003). [PubMed: 12955296]
52. Ranade SS et al. , Piezo2 is the major transducer of mechanical forces for touch sensation in mice. *Nature* 516, 121–U330 (2014). [PubMed: 25471886]
53. Iyer SH et al. , Progressive cardiorespiratory dysfunction in Kv1.1 knockout mice may provide temporal biomarkers of pending sudden unexpected death in epilepsy (SUDEP): The contribution of orexin. *Epilepsia* 61, 572–588 (2020). [PubMed: 32030748]
54. Takao K, Miyakawa T, Light/dark transition test for mice. *J Vis Exp*, 104 (2006). [PubMed: 18704188]
55. Shepherd JK, Grewal SS, Fletcher A, Bill DJ, Dourish CT, Behavioural and pharmacological characterisation of the elevated "zero-maze" as an animal model of anxiety. *Psychopharmacology (Berl)* 116, 56–64 (1994). [PubMed: 7862931]
56. Moy SS et al. , Mouse behavioral tasks relevant to autism: phenotypes of 10 inbred strains. *Behav Brain Res* 176, 4–20 (2007). [PubMed: 16971002]
57. Zhao ZQ et al. , Cross-inhibition of NMBR and GRPR signaling maintains normal histaminergic itch transmission. *J Neurosci* 34, 12402–12414 (2014). [PubMed: 25209280]
58. Zeng WB et al. , Anterograde monosynaptic transneuronal tracers derived from herpes simplex virus 1 strain H129. *Mol Neurodegener* 12, 38 (2017). [PubMed: 28499404]
59. Wan L et al. , Distinct roles of NMB and GRP in itch transmission. *Sci Rep* 7, 15466 (2017). [PubMed: 29133874]
60. Allard J, Physiological properties of the lamina I spinoparabrachial neurons in the mouse. *J Physiol* 597, 2097–2113 (2019). [PubMed: 30719699]
61. Cuellar JM, Antognini JF, Carstens E, An in vivo method for recording single unit activity in lumbar spinal cord in mice anesthetized with a volatile anesthetic. *Brain Res Brain Res Protoc* 13, 126–134 (2004). [PubMed: 15171995]
62. Minett MS et al. , Endogenous opioids contribute to insensitivity to pain in humans and mice lacking sodium channel Nav1.7. *Nature communications* 6, 8967 (2015).
63. Loken LS, Evert M, Wessberg J, Pleasantness of touch in human glabrous and hairy skin: order effects on affective ratings. *Brain research* 1417, 9–15 (2011). [PubMed: 21907328]
64. Ackerley R et al. , An fMRI study on cortical responses during active self-touch and passive touch from others. *Front Behav Neurosci* 6, 51 (2012). [PubMed: 22891054]
65. Leem JW, Willis WD, Chung JM, Cutaneous sensory receptors in the rat foot. *Journal of neurophysiology* 69, 1684–1699 (1993). [PubMed: 8509832]
66. Bessou P, Burgess PR, Perl ER, Taylor CB, Dynamic properties of mechanoreceptors with unmyelinated (C) fibers. *J Neurophysiol* 34, 116–131 (1971). [PubMed: 5540574]
67. Carcea I et al. , Oxytocin neurons enable social transmission of maternal behaviour. *Nature* 596, 553–557 (2021). [PubMed: 34381215]
68. Watkins RH et al. , Optimal delineation of single C-tactile and C-nociceptive afferents in humans by latency slowing. *J Neurophysiol* 117, 1608–1614 (2017). [PubMed: 28123010]

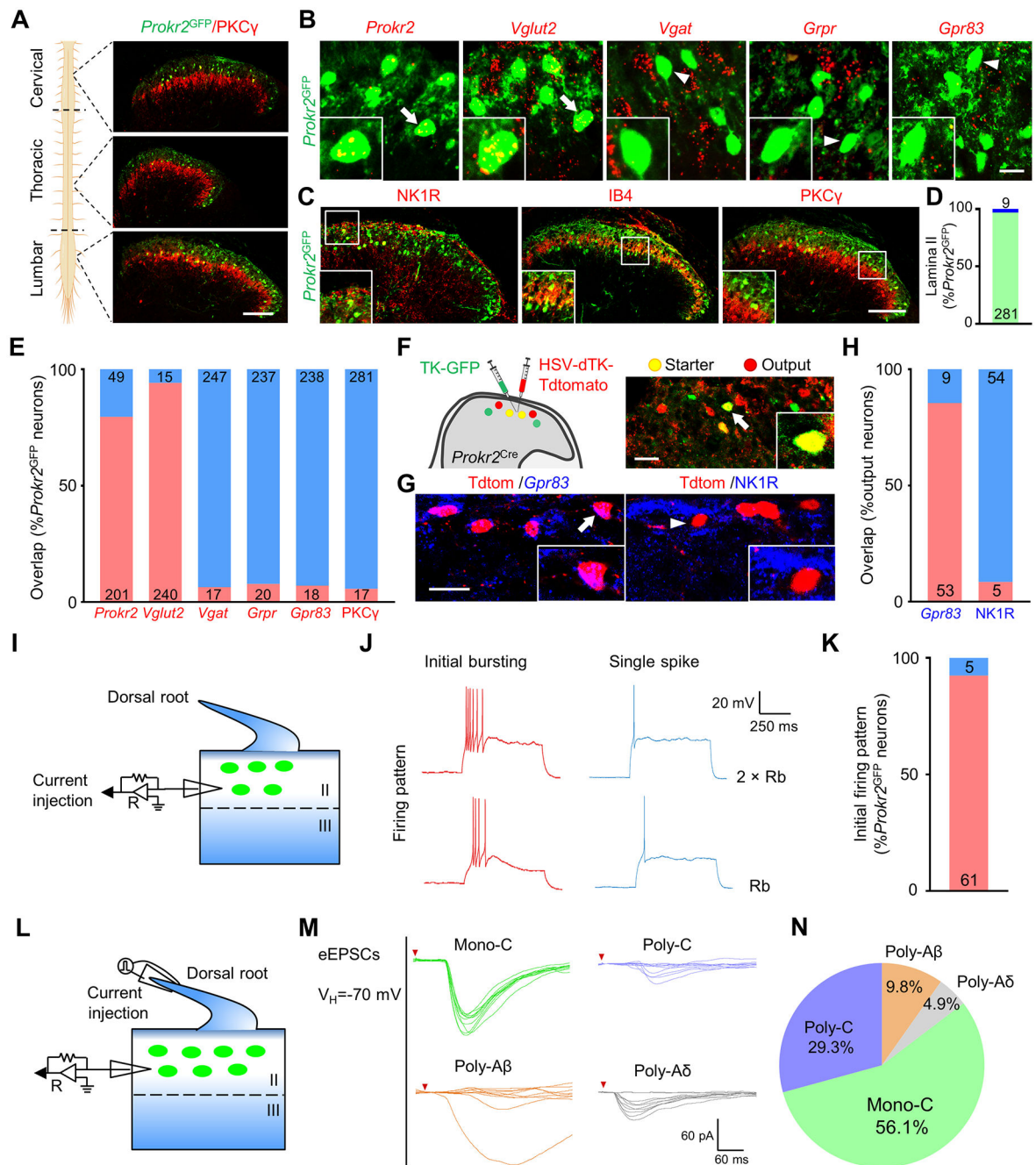


Fig. 1. PROKR2 neurons are a unique population of spinal excitatory interneurons.

(A to E) Double staining of GFP with PKC γ at three levels of the spinal cord (A); GFP with various markers in the lumbar cord (B), (C). Arrows: double-labeled cells. Arrowheads: GFP only. $n = 3$. Scale bar, 100 μ m for (A), (C), 20 μ m for (B). (D), Quantification of (C), percentage of *Prokr2^{GFP}* cells in lamina II (green) and lamina I (blue). (E), Quantification of (B), (C). Red in (E): percentage of double-labeled cells of *Prokr2^{GFP}* cells; blue: GFP only. (F) Schematic of intraspinal injection of virus AAV5-Ef1a-DIO-EGFP-2a-TK-WPRE-pA (TK-GFP) and HSV-dTK-LSL-tdTomato (HSV-dTK-Tdtomato) in the dorsal horn of *Prokr2^{Cre}* mice at the lumbar level (left); Image showing virus expression in a starter neuron

(yellow) expressing GFP and Tdtomato (right). Scale bar, 20 μm . **(G)** Double staining of *Gpr83* or NK1R anterogradely labeled with Tdtomato. **(H)** Quantification of **(G)**, $n = 3$. Scale bar, 20 μm . **(I to K)** Schematic of the whole-cell patch-clamp recording of *Prokr2*^{GFP} neurons in the spinal cord slice preparations **(I)**, a representative trace of initial firing pattern (red) and single spike firing pattern (blue) at 20 pA (rheobase or Rb) and 40 pA (2-fold rheobase or $2 \times \text{Rb}$) **(J)** and proportions of different types of firing pattern **(K)**. $n = 66$ neurons. **(L to N)** Schematic of the recording of the type of inputs onto *Prokr2*^{GFP} neurons with dorsal root stimulation **(L)**, representative traces of different types of inputs **(M)** and their proportions **(N)**. $n = 41$ neurons. All data are presented as mean \pm s.e.m.

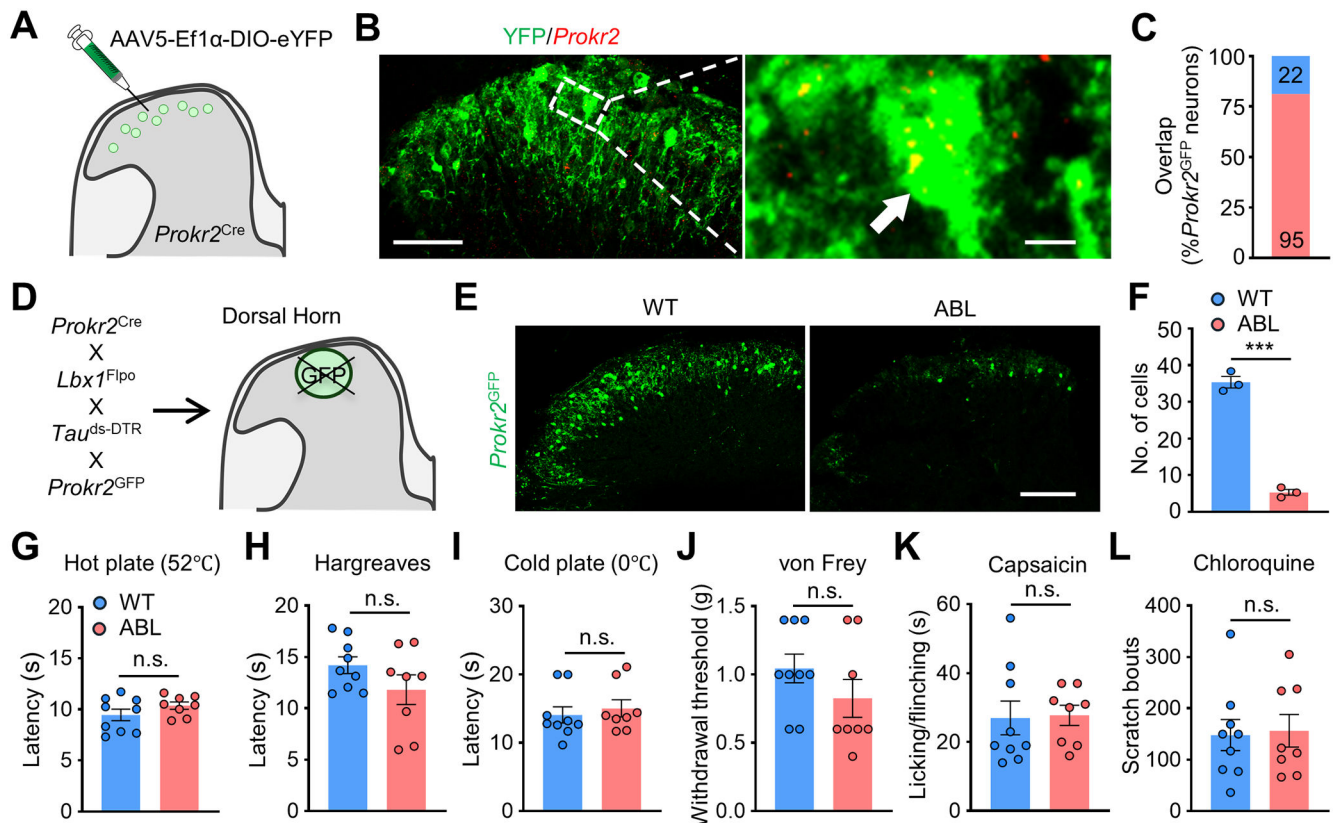


Fig. 2. PROKR2 neurons are dispensable for acute pain and itch transmission.

(A) Schematic of intraspinal injection of Cre-dependent AAV virus expressing YFP. (B and C) Double staining of YFP and *Prokr2* (Arrow: a double-stained cell) in the lumbar cord (B) and percentage of overlapping cells (C). Scale bar, 50 μm (left), 5 μm (right). (D) Strategy for intersectional genetic ablation of spinal *Prokr2*^{Cre} neurons. *Prokr2*^{Cre} mice were mated with *Lbx1*^{Flpo}, *Tau*^{ds-DTR}, *Prokr2*^{GFP} lines to generate diphtheria toxin receptor (DTR)-expressing *Prokr2* neurons by injection of diphtheria toxin (50 $\mu\text{g}/\text{kg}$, i.p.). (E and F) Images of *Prokr2*^{GFP} neurons in WT and ABL mice (E) and quantification of *Prokr2*^{GFP} neurons of (E) (F). Scale bar, 150 μm . (G to L) Comparable latencies in hot plate (G), Hargreaves (H), cold plate (I) tests, withdraw threshold in von Frey test (J), licking/flinching time induced by capsaicin (2 g, i.pl.) (K) and scratching numbers induced by chloroquine (200 μg , i.d.) (L) between WT and ABL mice. i.p., intraplantar injection. i.p., intraperitoneal injection, i.d., intradermal injection. WT, wild-type; ABL, mice with ablation of spinal *Prokr2* neurons; $n = 3$ for (F), $n = 8\text{--}9$ for (G to L); unpaired *t*-test in (F), (G to I); *** $P < 0.001$. n.s. – not significant. Error bars indicate s.e.m.

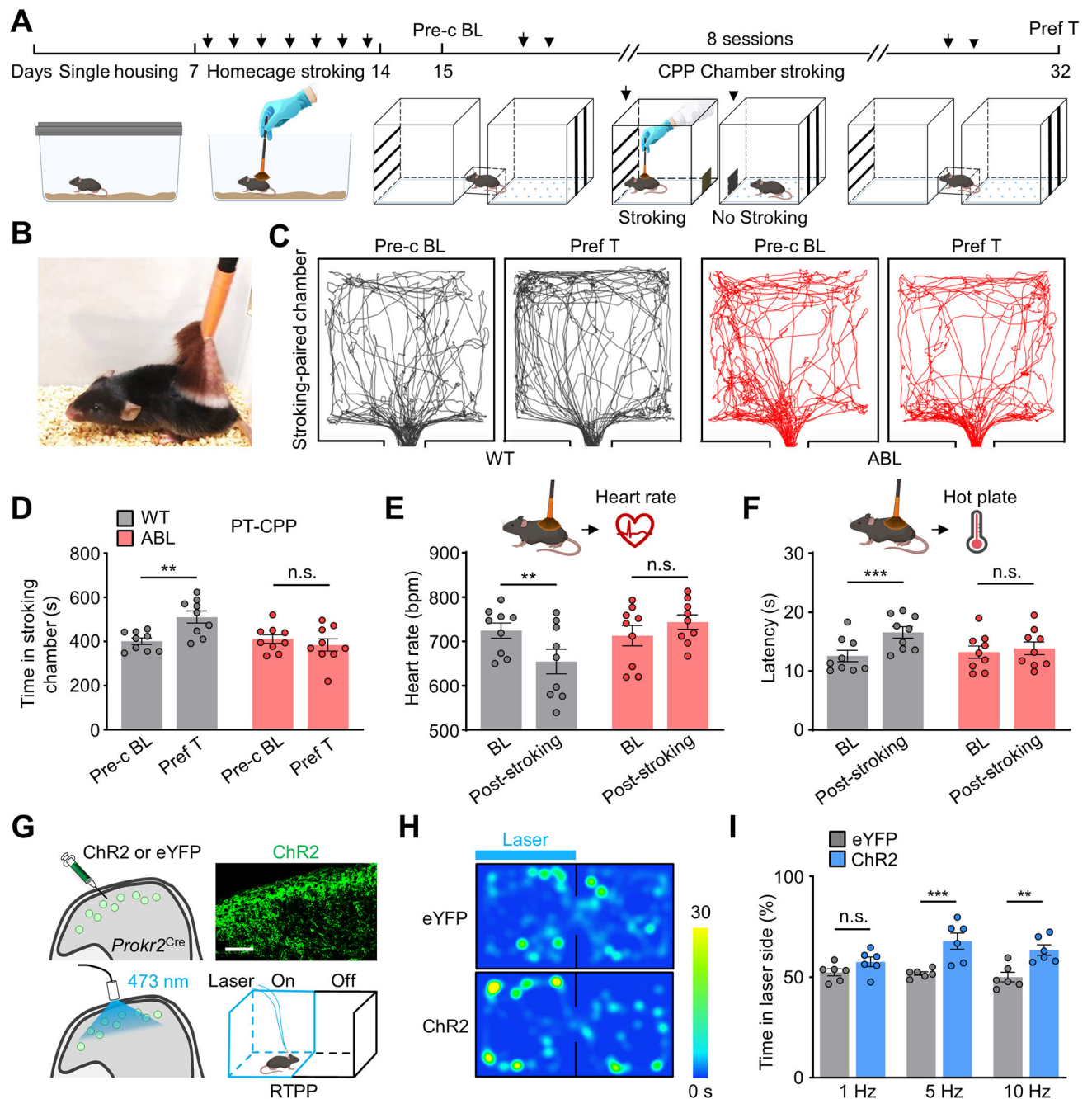


Fig. 3. PROKR2 neurons transmit pleasant touch sensation.

(A) A schematic diagram of the experimental procedure for PT-CPP. (B) Photo of a mouse being stroked with a soft brush. (C and D) Representative trajectory plot (C) and time spent (D) in stroking-paired chamber for WT and ABL mice in the pre-conditioning baseline (Pre-c BL) and preference test (Pref T). Pre-c BL versus Pref T, $P < 0.01$ for WT and $P = 0.6822$ for ABL mice. (E and F) Heart rate (E) and thermal pain threshold (F) in the baseline and post-stroking test. Heart rate, BL versus post-stroking, $P < 0.01$ for WT and $P = 0.1563$ for ABL mice; hot plate, BL versus post-stroking, $P < 0.001$ for WT and $P = 0.5206$ for ABL mice. (G) Schematic of intraspinal injection of Cre-dependent AAV virus

expressing ChR2-eYFP or eYFP (top, left) and image showing ChR2-eYFP in the cervical cord (top, right). Schematic of real-time place preference test (RTPP) (bottom). Scale bar, 50 μm . **(H and I)** Representative heat map (5 Hz) (**H**) and the percentage of time spent (**I**) in the chamber paired with the laser in the RTPP test. $n = 9$ for (**D to F**), $n = 6$ for (**I**); two-way repeated measures ANOVA followed by Bonferroni's multiple comparisons test in (**D**), (**E**), (**F**), two-way ANOVA followed by Bonferroni's multiple comparisons test in (**I**); ** $P < 0.01$, *** $P < 0.001$. n.s. – not significant. Error bars indicate s.e.m.

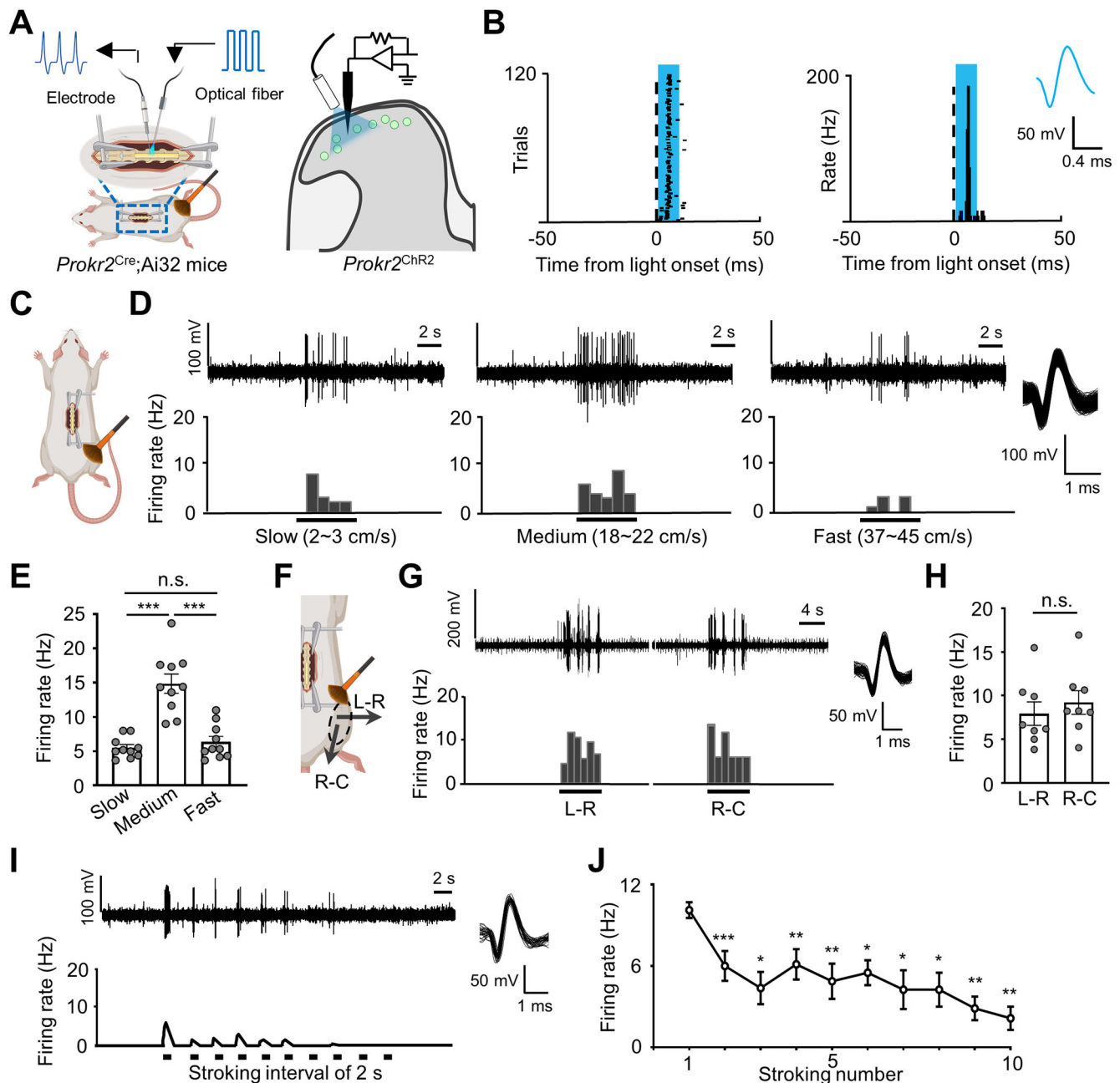


Fig. 4. PROKR2 neurons display characteristic features in response to gentle stroking.

(A) Left, dorsal view of an anesthetized *Prokr2^{Cre};Ai32* mouse showing the position of optical fiber and electrode implanted in the lumbar spinal cord. Right, cross-section view of the lumbar spinal cord showing optogenetic tagging of *Prokr2^{ChR2}* neurons in lamina II with blue lights on. (B) Example response of a PROKR2-expressing neuron to blue light activation. Left, spike raster showing multiple trials of laser stimulation at 1 Hz. Right, the firing rate of one opto-tagged neuron within 10 ms light pulses. Inset, waveform on expanded time scale. Blue bar, light pulse. (C to E) Schematic of brush stroking across the receptive field (C), representative traces (top) and corresponding peristimulus time histogram (PSTH, 1 s bin) (bottom) (D), and firing rate (E) of *Prokr2^{ChR2}* neurons in

response to a soft brush stroking moving at different speeds (slow, 2~3 cm/s; medium, 18~22 cm/s; fast, 37~45 cm/s) cross the receptive field of hindlimb hairy skin. Dots represent spike rate of a single trial from individual neurons (E). (F to H) Schematic of brush stroking in different directions ((F), L-R: from left to right; R-C: from rostral to caudal), representative traces (top), corresponding PSTH (1s bin, bottom) (G) and firing rate (H) of spinal *Prokr2^{ChR2}* neurons in response to stroking in different directions. Brush stroking was applied across the receptive field of the hindlimb in different directions at a speed of 18~22 cm/s. (I and J) Representative trace (top), corresponding PSTH (1s bin, bottom) (I) and firing rate (J) of spinal *Prokr2^{ChR2}* neurons in response to 10 repeated brush stroking stimuli with intervals of 2 s. Inset, superimposed waveforms on expanded time scale representing spikes of *Prokr2^{ChR2}* neurons evoked by stroking in (D), (G), (I). $n = 8\sim 10$ neurons from 3~4 mice; one-way repeated measures ANOVA followed by Bonferroni post hoc in (E), (J), paired t -test in (H); * $P < 0.05$, ** $P < 0.01$, *** $P < 0.001$. n.s. – not significant. Error bars indicate s.e.m.

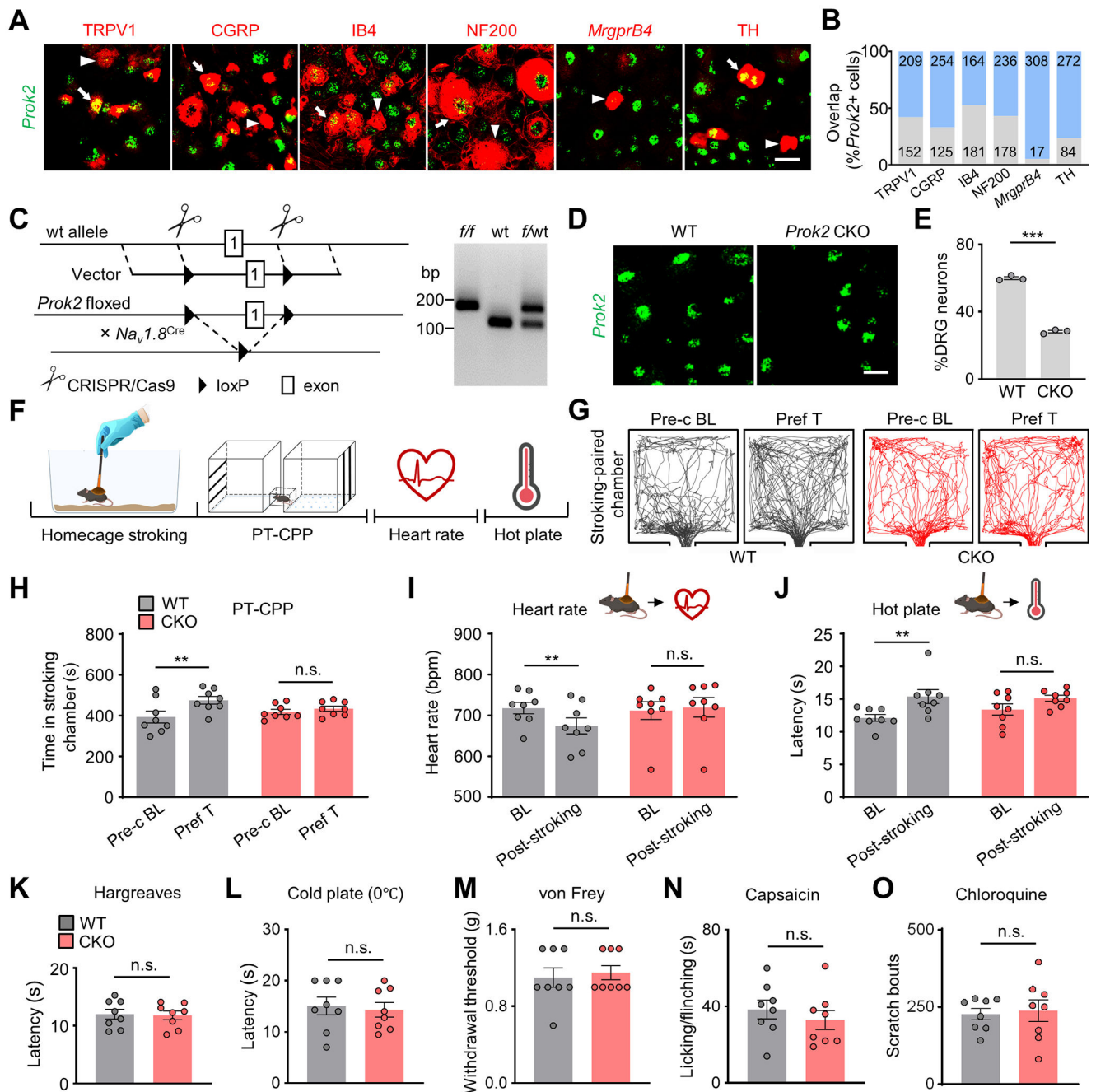


Fig. 5. Conditional deletion of *Prok2* in sensory neurons abolishes pleasant touch sensation. (A) Double staining of *Prok2* with various markers in DRG neurons. Arrows: double-stained cells; arrowheads: *Prok2* cells only. TH, tyrosine hydroxylase. (B) Overlapping percentages of (A). Grey: double-stained ratio; blue: *Prok2* only. Scale bar, 20 μ m. (C) Left, schematic of targeting strategy for generating *Prok2* floxed (*Prok2*^{f/f}) mice which were mated with *Nav1.8*^{Cre} mice to generate *Prok2*^{f/f};*Nav1.8*^{Cre} mice or *Prok2* CKO mice. Right, Gel electrophoresis of genotyping PCR from *Prok2*^{f/f}, wt/wt and *Prok2*^{f/wt} samples. (D) Expression of *Prok2* in DRGs of the control (*Prok2*^{f/f}, WT) and *Prok2* CKO mice (*Prok2*^{f/f};*Nav1.8*^{Cre}, CKO). (E) Quantification of (D). Scale bar, 20 μ m. (F) A schematic of

the experimental procedure. Parallel symbols indicate that PT-CPP, heart rate and hot plate tests were performed independently following single housing and homecage stroking. (**G** and **H**) Representative trajectory plot (**G**) and time spent (**H**) in stroking-paired chamber for WT and CKO mice in the pre-conditioning baseline (Pre-c BL) and preference test (Pref T). Pre-c BL versus Pref T, $P < 0.01$ for WT and $P = 0.9552$ for CKO mice. (**I** and **J**) Heart rate test (**I**) and hot plate test (**J**) in WT and CKO mice. Heart rate, BL versus post-stroking, $P < 0.01$ for WT and $P = 0.8737$ for CKO mice; hot plate, BL versus post-stroking, $P < 0.01$ for WT and $P = 0.1531$ for CKO mice. (**K** to **O**) Comparable latencies in Hargreaves test (**K**), cold plate test (**L**), withdraw threshold in von Frey test (**M**), licking/flinching time induced by capsaicin (2 g, i.pl.) (**N**) and scratching numbers induced by Chloroquine injection (200 μ g, i.d.) (**O**) between WT and CKO mice. WT, wild-type; CKO, *Prok2*CKO mice. $n = 3$ for **e**, $n = 8$ for (**H**) to (**O**); unpaired *t*-test in (**E**), (**K**)-(O), two-way repeated measures ANOVA followed by Bonferroni's multiple comparisons test in (**H**), (**I**), (**J**); ** $P < 0.01$, *** $P < 0.001$. n.s. – not significant. Error bars indicate s.e.m.

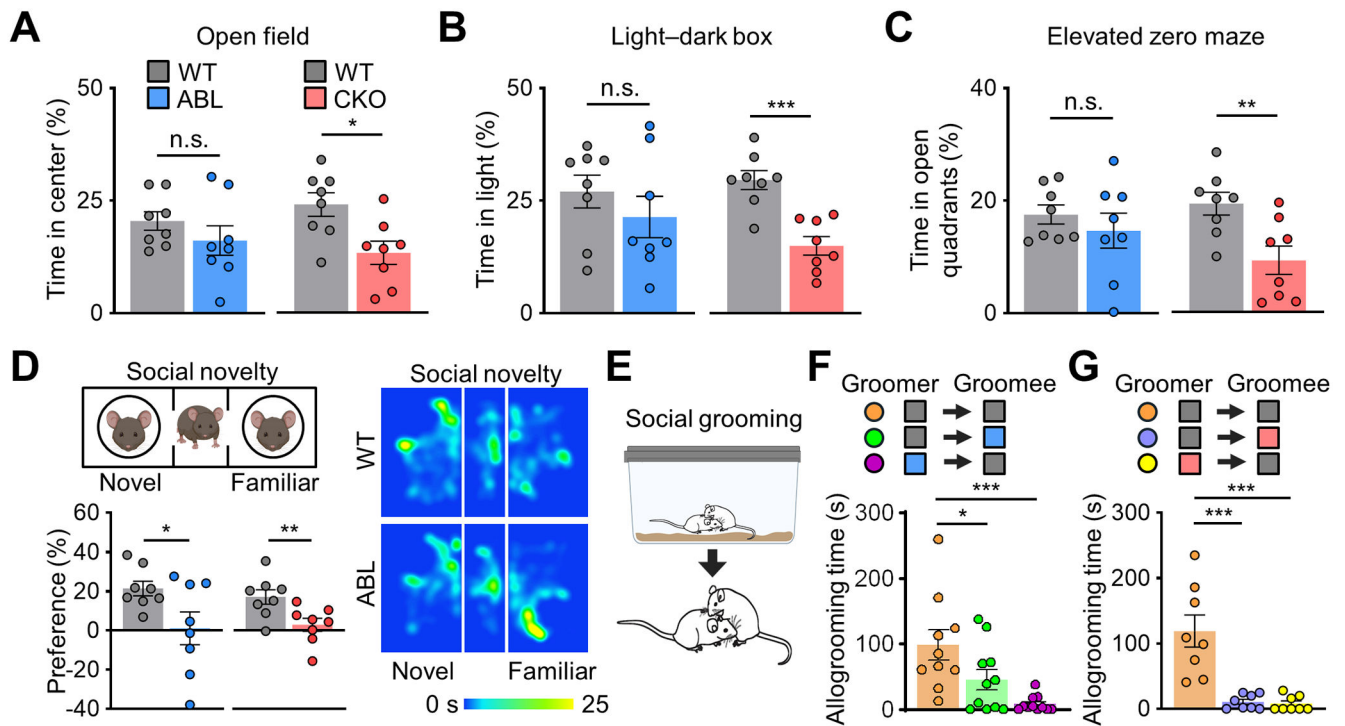


Fig. 6. Profound impairments of PROR2/PROKR2 mutant mice in stress response and prosocial behaviors.

(A to C) Stress and anxiety-like behavioral tests. The percentage of time spent in the center zone of the open field apparatus (A), light illuminated chamber of the light-dark box (B) and the open quadrants of the elevated zero maze (C). WT versus ABL, $P = 0.2795$ (A); $P = 0.3514$ (B); $P = 0.4312$ (C). WT versus CKO, $P < 0.05$ (A); $P < 0.001$ (B); $P < 0.01$ (C). (D) The three-chamber social novelty test. The preference index for the percentage of time spent exploring the chamber with a novel mouse versus a familiar mouse (left). Right, representative heat maps of locomotor activity in the chambers. WT versus ABL, $P < 0.05$; WT versus CKO, $P < 0.01$. (E-G) The homecage social grooming test. Cartoons showing mouse allogrooming in the homecage (E). (F and G) Allogrooming time for each pair. Groomer-groomee (F), WT-WT pair versus WT-ABL pair, $*P < 0.05$; WT-WT pair versus ABL-WT pair, $***P < 0.001$. Groomer-groomee (G), WT-WT pair versus WT-CKO pair, $***P < 0.001$; WT-WT pair versus CKO-WT pair, $***P < 0.001$. $n = 8$ for (A to D), (G), $n = 10\text{--}11$ for (F); unpaired t -test in (A to D), one-way ANOVA followed by Bonferroni post hoc in (F), (G); $*P < 0.05$, $**P < 0.01$, $***P < 0.001$. n.s. – not significant. Error bars indicate s.e.m.